ELSEVIER

Biochimica et Biophysica Acta 1232 (1995) 197–207

BBA Biochimica et Biophysica Acta

Microscopic and spectroscopic studies of untreated and hexanol-treated chlorosomes from *Chloroflexus aurantiacus*

Yinwen Zhu [a,b], B.L. Ramakrishna [a], Paula I. van Noort [a,b], Robert E. Blankenship [a,b,*]

[a] *Department of Chemistry and Biochemistry, Arizona State University, Tempe, AZ 85287-1604, USA*
[b] *Center for the Study of Early Events in Photosynthesis, Arizona State University, Tempe, AZ 85287-1604, USA*

Received 27 January 1995; accepted 3 August 1995

Abstract

When isolated chlorosomes from *Chloroflexus aurantiacus* are treated with 1-hexanol, the BChl *c* Q_y absorption band shifts from 740 to 670 nm, while the baseplate BChl *a* remains at 795 nm. The relative amount of BChl *c* in the 740 and 670 nm forms depends on the hexanol concentration. Atomic force microscopy was used to study the ultrastructure of native, hexanol-treated, and protein-free chlorosomes. Chlorosomes appeared to be larger and more rounded upon hexanol treatment and did not return to the original shape or size after 2-fold dilution. Therefore, the hexanol treatment is not completely reversible in terms of chlorosome structure. Untreated, hexanol-treated and and hexanol-treated and then diluted samples were investigated using steady-state and time-resolved fluorescence spectroscopy. For the sample treated with 68 mM hexanol, a 24 ps energy transfer from BChl *c* to *a* was observed in the picosecond fluorescence measurements. After 2-fold dilution, most of the kinetic properties of the untreated chlorosomes, characterized by a major energy transfer component of 15 ps from BChl *c* 740 to BChl *a* 795, were regained. Energy transfer from either BChl *c* 740 or BChl *c* 670 to baseplate BChl *a* is fast and relatively efficient in untreated chlorosomes. In hexanol-treated chlorosomes, the excited state lifetime is not very different from that in untreated samples, but the energy transfer efficiency is quite low. This may result from concentration quenching of the monomeric pigments in the hexanol-treated chlorosomes.

Keywords: Chlorosome; Energy transfer; Hexanol; Ultrastructure; Photosynthesis; Atomic force microscopy; Bacteriochlorophyll

1. Introduction

The major light-harvesting structures in green photosynthetic bacteria are chlorosomes, which are oblong bodies attached to the cytoplasmic side of the cell membrane [1–5]. In the green gliding bacterium *Chloroflexus aurantiacus*, the chlorosome is approximately 100 nm long, 30 nm wide and about 10 nm thick, and is surrounded by a lipid monolayer [6]. It contains BChl *c* aggregates and carotenoids, as well as a small amount of BChl *a* [7–9]. Three major polypeptides [10], namely, 18, 11 and 5.7 kDa polypeptides, have been found to be associated with chlorosomes, but their functions are still unclear.

The most abundant pigment in chlorosomes from *Cf. aurantiacus* is BChl *c*, with about 10000 molecules in each antenna structure. The Q_y absorption band of BChl *c* in the chlorosome is about 70–80 nm red-shifted as compared to the monomeric form. The kinetics of energy transfer within chlorosomes from various species have been extensively investigated (see [1–5] for reviews) both experimentally [11–19] and theoretically [20]. Steady-state fluorescence studies [9], [21] suggested an energy transfer pathway from BChl *c* aggregates to BChl *a* in a so-called baseplate structure [6], which further connects to a BChl *a*-protein complex, B808-866 in the membrane. Some minor forms of BChl *c* and *a* pigments may also play a role in mediating certain energy flow steps [22], [19]. Overall, the excited state of BChl *c* is found to decay with a lifetime of about 10–20 ps in isolated chlorosomes [11–19]. However, recent measurements on the subpi-

Abbreviations: BChl, bacteriochlorophyll; Cf., *Chloroflexus*; AFM, atomic force microscopy; ETE, energy transfer efficiency; ps, picosecond; fs, femtosecond; LD, linear dichroism; SPC, single photon counting; SDS, sodium dodecyl sulfate; LDS, lithium dodecyl sulfate.

* Corresponding author. Address a. Fax: +1 602 9652747. E-mail: Blankenship@asu.edu.

SSDI 0005-2728(95)00118-2

cosecond timescale have revealed ultrafast components in the BChl *c* decay [19].

Questions remain on the organization of BChl *c* in chlorosomes. It was proposed to bind to the 5.7 kDa protein [23], in which case the protein would play a major functional role [24]. Other evidence, however, argues against this conclusion. Also, when chlorosomes are treated with the detergent sodium dodecyl sulfate, which removes all the proteins, BChl *c* shows similar spectral properties to those of untreated samples [25]. Other studies showed that BChl *c* can associate spontaneously in non-polar solvents [26–29] aqueous solutions [30,31] or detergent suspensions ([32], and Van Noort, P.I., unpublished data). All these protein-free aggregates have a BChl *c* absorption almost identical to that of native chlorosomes. Based on the idea that proteins are not required for formation of the 740–750 nm absorbing species in chlorosomes, different models for BChl *c* organization have been proposed [26,27,33–38]. In these models, the central Mg is thought to be essential for the aggregation, bridging neighboring pigments. Two of the functional groups of BChl *c*, the 3^1-hydroxyl and 13^1-keto groups, are involved in the oligomer formation, although the precise geometry of the oligomers are not known.

Efforts were also made by various groups to chemically treat the native chlorosome to study the BChl *c* organization indirectly. One interesting chemical is 1-hexanol, which has a six-carbon hydrophobic chain and a hydroxyl group. It was first reported by Brune et al. [11] that the 740 nm absorbing form of BChl *c* in the *Chloroflexus* chlorosome can be converted to a 670 nm absorbing form by the addition of 1% 1-hexanol to the chlorosome solution. The effect was partially reversible by dilution with buffer. Matsuura and Olson [39] showed that the hexanol effect can be completely reversible, based on steady-state fluorescence and absorption results. Linear dichroism (LD) studies [40] suggested that BChl *c* loses its orientation upon hexanol treatment, but is still organized in a somewhat ordered form. Miller et al. [31] further found that the absorption spectrum of an aqueous aggregate of BChl *c* can also be reversibly converted to the 670 nm form by hexanol.

In this paper, we examined the size and shape of native, hexanol-treated, and protein-free chlorosomes using atomic force microscopy [41]. We also report the steady-state and time-resolved fluorescence and absorption difference spectral measurements of chlorosome samples treated with different concentrations of hexanol.

2. Materials and methods

2.1. Cell growth and chlorosome purification

Chloroflexus aurantiacus was grown photoheterotrophically in 1-liter batch cultures at 55°C as described by Pierson and Castenholz [42]. The cells were harvested by centrifugation after 3–4 days of growth and chlorosomes were isolated by the method of Gerola and Olson [43] using a 2 M concentration of the chaotropic agent, NaSCN. After a 10–50% linear sucrose gradient ultracentrifugation, the chlorosome band was collected for spectroscopic studies.

2.2. Hexanol treatment

A hexanol solution was prepared by adding 0.6–0.85% (v/v) 1-hexanol to 10 mM phosphate buffer (pH 7.4) and shaking vigorously. The hexanol-buffer mixture was then allowed to stand at room temperature for 20–30 min. Concentrated chlorosomes were diluted into the hexanol-containing buffer. The final concentration of hexanol was estimated to be 48–68 mM. To reverse the hexanol effect, fresh buffer was added slowly (dropwise) to the treated sample.

2.3. Atomic force microscopy (AFM)

All the samples for AFM were diluted to a final optical density of about 0.1 at 740 nm or 670 nm for the hexanol-treated samples. In the detergent treatment, 1% (w/v) sodium dodecyl sulfate was mixed with the chlorosome sample, and incubated at 50°C for 20 min. In order to remove the detergent which may interfere with the chlorosome image in AFM pictures, the sample was centrifuged at $150\,000 \times g$ for 1 h and the pellet was collected and dissolved in H_2O.

Discs of muscovite mica, a few tenths of a millimeter thick, were first glued to magnetic stainless steel punches and then cleaved to expose a fresh clean surface. An aliquot of approximately 20 μl of each sample was immediately pipetted onto the surface and dried in air overnight. The surface of the mica was rinsed with water (or hexanol-containing water) and left to dry again. For the untreated chlorosome sample, a 20 nm thick carbon amorphous layer was applied on the sample surface in a vacuum chamber.

The samples were imaged under ambient air conditions with a commercial AFM (Nanoscope III, Digital Instruments, CA). For the contact mode AFM, the cantilevers were 100 μm long, with a manufacturer's reported spring constant of 0.1 N/m. In order to minimize damage to the sample by the scanning probe, we also employed the TappingMode™ technique [44]. A stiff 125 μm silicon cantilever (spring constant was 50 N/m) with an integral tip was oscillated near its resonance frequency of about 300 kHz and the damping of the amplitude, which depends upon interaction with the sample and thus on the surface topography, was monitored with an optical laser beam and detector system.

In order to estimate the volume, all structures on AFM pictures were treated as ellipsoids. The equation $V =$

$(4/3)\pi abc$ was used, where a, b and c are radii of three dimensions.

2.4. Spectroscopy

Absorption spectra were measured on a Cary 5 spectrophotometer and steady-state fluorescence spectra were measured on a Spex Fluorolog 2.

Fluorescence lifetimes were measured using a single-photon counting instrument described earlier [45]. All the data reported in this paper were taken with 5 ps per channel over a 10 ns time scale. Fluorescence decays were detected at wavelengths between 660 and 830 nm, and global analyses were performed to generate decay-associated spectra.

3. Results

3.1. Atomic force microscopy (AFM)

We began our studies by examining the native chlorosome sample using tapping mode AFM. Carbon coating was applied to immobilize the sample surface. Fig. 1 is a typical 264 nm × 264 nm view of native chlorosomes. Panel a shows ellipsoidal bodies of a length of 90–110 nm and a width of about 30 nm. From panel b in Fig. 1, their thickness appears to be less than 10 nm. An average of 10 measured structures gave a chlorosome size of 99 nm long, 31 nm wide and 5 nm thick (Table 1).

Fig. 2 shows a 375 nm × 375 nm image of hexanol-treated chlorosomes obtained by tapping mode AFM. The structures seem to be much larger (Fig. 2a) and more

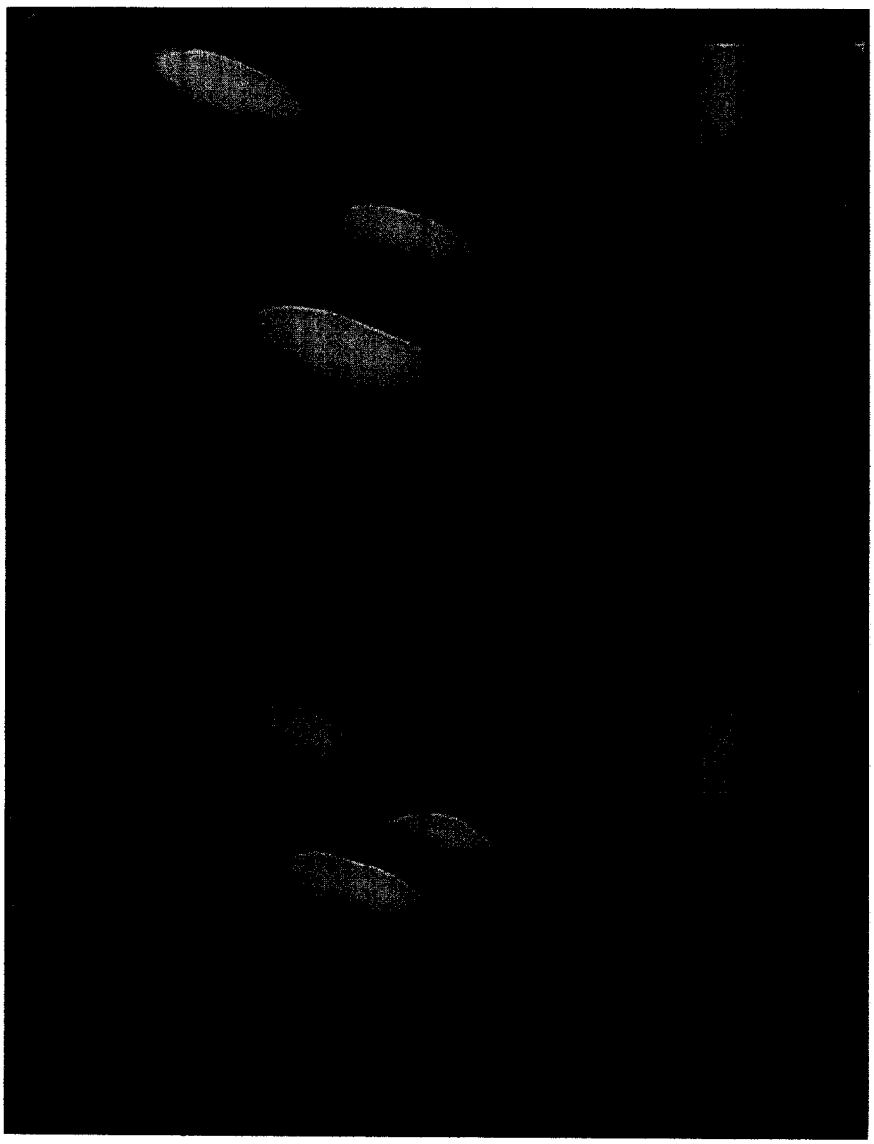

Fig. 1. Top view (a) and surface plot (b) of a tapping mode AFM image of an untreated chlorosome sample.

Table 1
Dimensions of chlorosome samples as determined by atomic force microscopy

[Hexanol] (mM)	Measured (nm) (±S.D.) length	width	height	volume ($\times 10^3$ nm^3)
0 (10) [a]	99 (±10)	31 (± 4)	5.0 (±0.6)	8.0
68 (10) [a]	179 (± 9)	99 (±11)	4.5 (±0.7)	41.7
34 (12) [a]	139 (±11)	115 (±12)	3.4 (±0.5)	28.5

[a] The number of chlorosome structures measured for averaging.

rounded (Fig. 2b) than native chlorosomes. An average length of 179 nm, width of 99 nm and thickness of 4.5 nm was obtained from 10 features.

When diluted 2-fold in H_2O, the chlorosomal vesicles (Fig. 3) became smaller than the treated ones in Fig. 2. They were estimated to be 139 nm long, 115 nm wide and 3.4 nm thick from averaging 12 structures. However, the structures are still considerably larger than the untreated chlorosomes.

After the native chlorosome sample was treated with 1% sodium dodecyl sulfate (SDS) for 20 min, the baseplate absorption around 795 nm disappeared, while the 740 nm BChl *c* band remained (data not shown). The chlorosomes were now free of proteins from the SDS-PAGE data ([32] and our results not shown here). We imaged the sample with the contact mode AFM [41]. The top view (Fig. 4a) shows near-circular features with a diameter range from 53–91 nm. This agrees with the results from a previous electron micrograph of lithium dodecyl sulfate (LDS)-treated samples [32]. However, according to the pictures in Fig. 4b, the structures are not spherical but disc-like, having an average thickness of 10 nm.

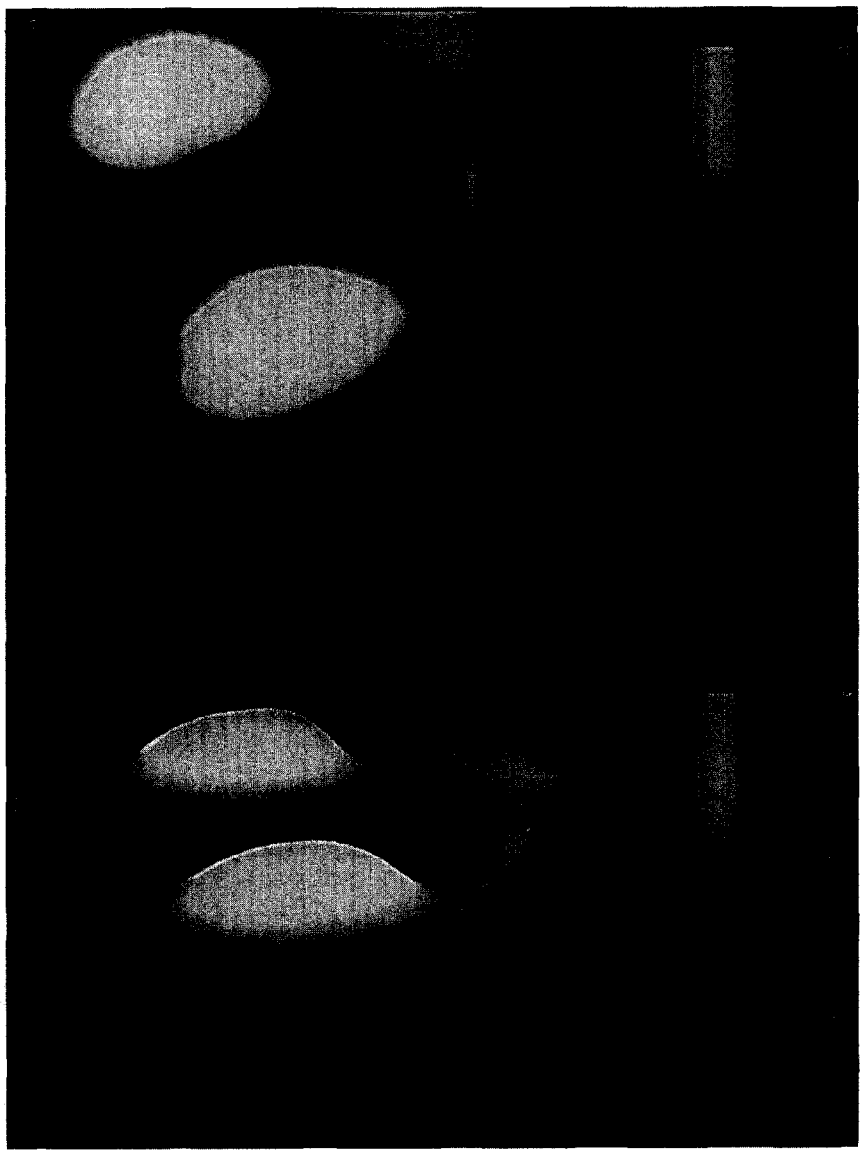

Fig. 2. Top view (a) and surface plot (b) of a tapping mode AFM image of a chlorosome sample containing 68 mM hexanol.

All the features in Fig. 1, Figs. 2 and 4 show a 'polished' surface topography, indicating a rather smooth exterior of the chlorosome envelope. In Fig. 3, however, the surface of the structures, as well as the background, give a rippled appearance. Although the cause is not known, we believe that this roughness does not reflect the real features of the sample.

3.2. Steady-state spectroscopy

Fig. 5 shows the steady-state absorption and fluorescence excitation and emission spectra of untreated and hexanol-treated chlorosomes. When chlorosomes were suspended in 68 mM hexanol, the BChl *c* absorption shifted from 740 nm to 670 nm, while the BChl *a* absorption of the baseplate remained unchanged (Fig. 5d). This is in agreement with previous observations [11], [39]. If the hexanol concentration was below 68 mM, only part of the BChl *c* 740 was converted to 670 nm form (Fig. 5b and c). When the hexanol concentration was increased from 48 to 68 mM, BChl *c* aggregate absorption around 740 nm shifted slightly to 730 nm, until it disappeared in 68 mM hexanol (Fig. 5d). When detected at 825 nm, the excitation spectrum of each sample showed peaks at 670 and 730–740 nm region. This indicated excited-state energy transfer from BChl *c*, both the 670 and 730–740 nm absorbing species, to the baseplate BChl *a*, absorbing around 790–795 nm. All the fluorescence emission spectra of hexanol-treated samples with excitation at 650 nm (Fig. 5b, c and d) showed a band around 800 nm. Since BChl *a* has essentially no absorption at 650 nm, this further confirms an energy transfer process from BChl *c* 670 to BChl *a*

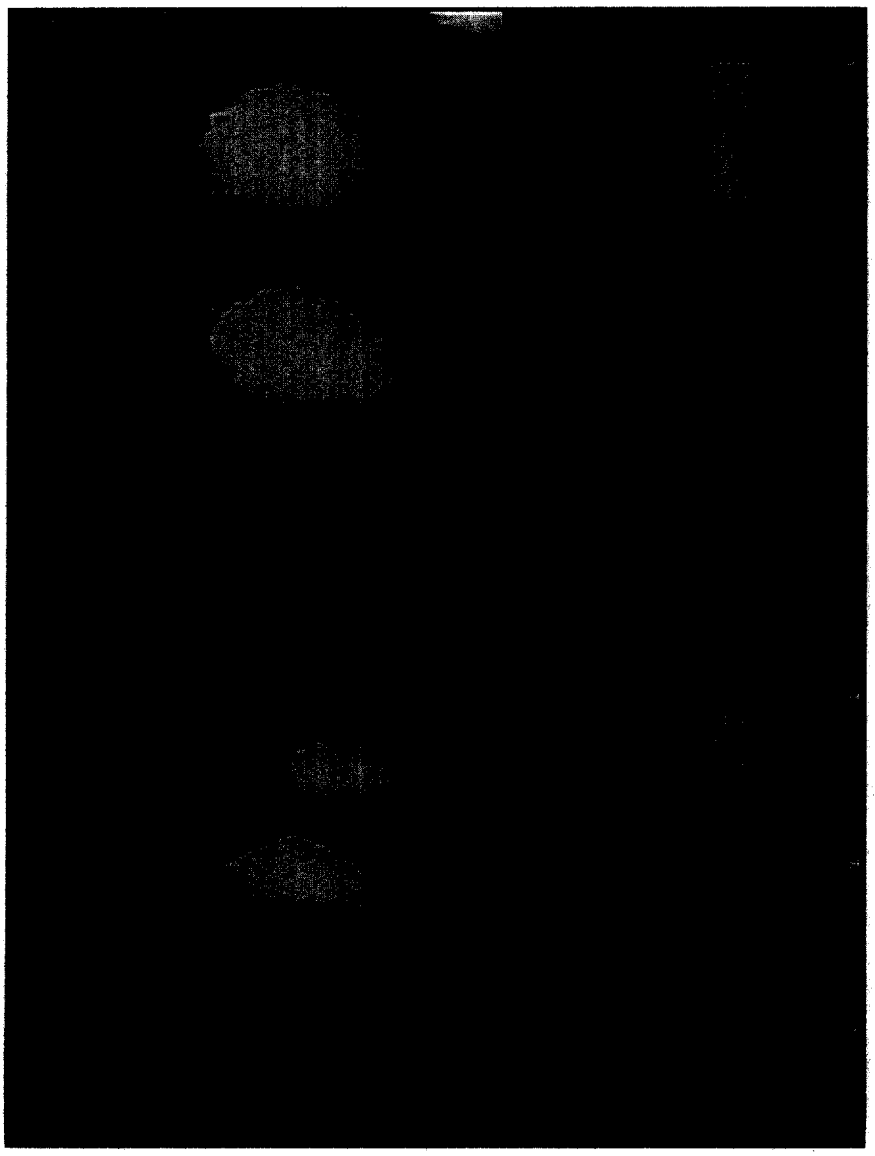

Fig. 3. Top view (a) and surface plot (b) of a tapping mode AFM image of chlorosomes in 34 mM hexanol buffer after dilution of chlorosomes in 68 mM hexanol.

795. Similarly, energy transfer from BChl *c* 670 to the baseplate BChl *a* was suggested in chlorosomes from *Chlorobium limicola* [39].

In Fig. 5, the absorption and fluorescence excitation spectra of each sample were normalized around 795 nm in order to visualize the energy transfer from BChl *c* to *a*. To calculate energy transfer efficiency (ETE), the excitation and the corresponding 1-transmittance spectra were compared, and the results are listed in Table 2. For untreated chlorosomes, the ETE from BChl *c* aggregate to BChl *a* in the baseplate was ~ 58%, which was comparable to the 55% observed earlier at both 77 K and room temperature [46]. Upon the addition of 56 mM hexanol, the ETE from 730–740 nm absorbing BChl *c* to BChl *a* decreased to 30%. This is about half that of the untreated chlorosome sample. On the other hand, as the hexanol concentration increased, the energy transfer from the 670 nm absorbing BChl *c* decreased almost 3-fold, from 36% to 13%. The relative amount of the 730–740 to 670 nm BChl *c* species also decreased in the same direction. These data suggest that the remaining 730–740 nm absorbing form of BChl *c* could function as an intermediate in the energy transfer pathway from 670 nm to 795 nm. In fact, when taking the excitation spectrum of the 68 mM hexanol-containing chlorosome sample with emission wavelength of 740 nm, we saw an absorption peak around 670 nm (data not shown), indicating that the 730–740 nm BChl *c* form accepts energy from BChl *c* 670.

3.3. Single photon counting fluorescence experiments

Matsuura and Olson [39] found that when the hexanol-treated chlorosome sample was diluted 2–3-fold with fresh buffer, it showed similar steady-state absorption and fluo-

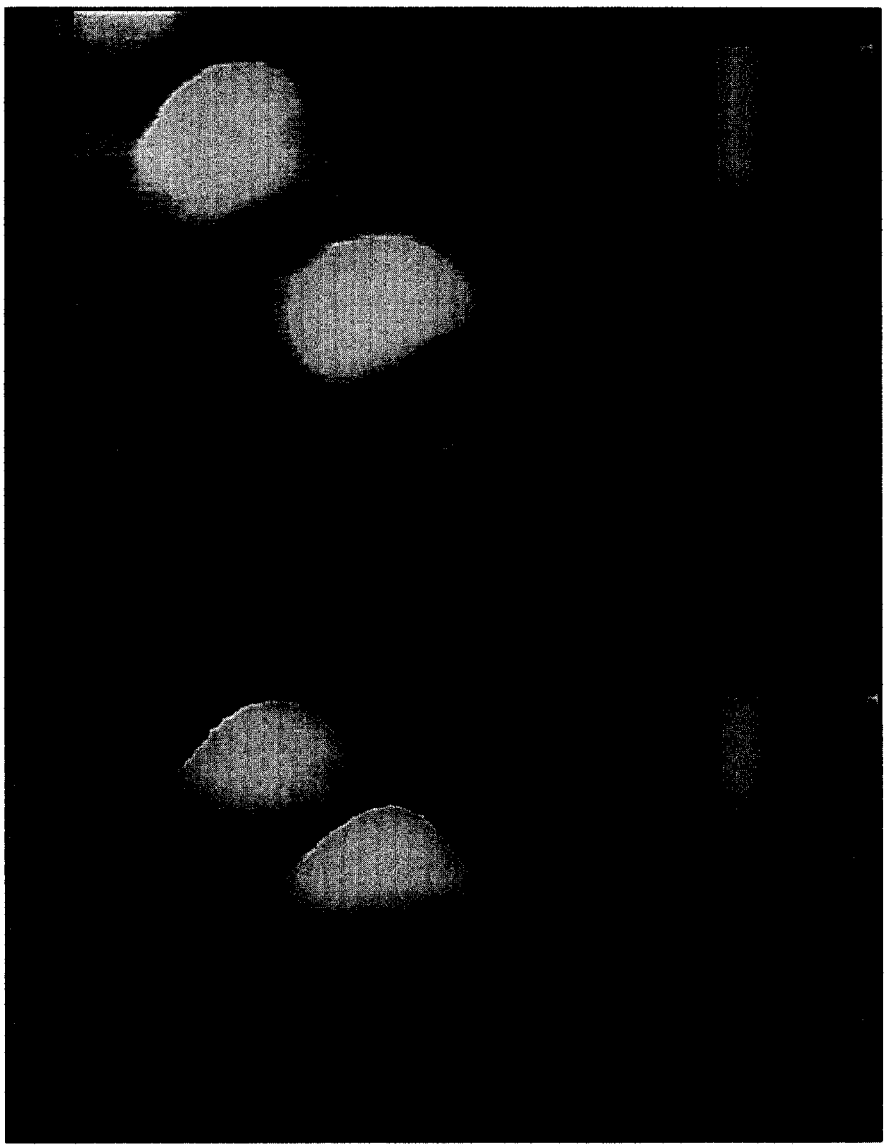

Fig. 4. Top view (a) and surface plot (b) of a regular AFM image of chlorosomes treated with 1% SDS.

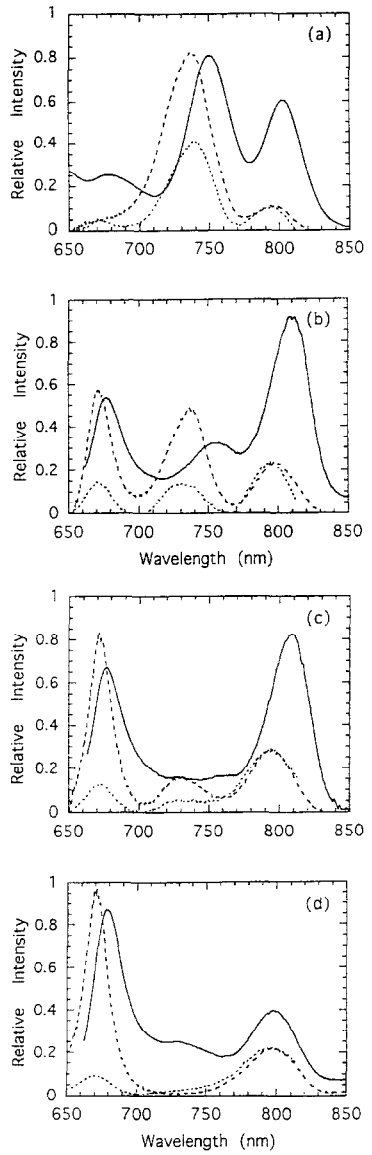

Fig. 5. Absorption (---), fluorescence excitation (· · ·) and emission (——) spectra of untreated (a) and hexanol-treated chlorosomes (b, c and d). Hexanol concentrations were 48 mM (b), 56 mM (c), and 68 mM (d), respectively. Fluorescence emission spectra were taken with excitation at 650 nm for (b), (c), (d) and 460 nm for (a). Fluorescence excitation spectra were detected at 825 nm for all samples. Absorption and corresponding excitation spectra were normalized at about 795 nm.

rescence emission spectra as compared to untreated chlorosomes. To test the reversibility in terms of kinetics, single-photon counting experiments were performed on native, hexanol-containing, and hexanol-recovered chlorosomes from the same preparation. Decay-associated emission spectra (DAS) of the different chlorosomes are shown in Fig. 6. A sum of five exponentials was used to fit decay curves at 11 wavelengths for native, 48 mM hexanol-treated and recovered chlorosomes, respectively, and at 12 wavelengths for 68 mM hexanol-treated chlorosomes. Compared to that of four exponentials, the five exponential analysis gave a much better global fit in most cases based on the residuals at certain wavelengths and the overall χ^2. For example, the χ^2 of the global analysis shown in Fig. 6b was 1.21, much lower than the 1.64 if four lifetimes were used.

The most dominant component in all the spectra is the fast component which changes its amplitude from positive to negative with increasing wavelength. This component represents an energy transfer from BChl *c* to BChl *a* 795, with positive amplitudes for the decay of the BChl *c* emission and negative amplitudes for the rise of the BChl *a* 795 emission. Samples in Fig. 6a and d, which are untreated and hexanol-recovered chlorosomes, respectively, display very similar global analysis kinetics. A major lifetime of 15–17 ps was observed for both the untreated and recovered samples. A minor difference is that the center of the negative band around 800 nm is slightly blue-shifted for the 15–17 ps fast component for the recovered chlorosomes.

In order to investigate the energy transfer pathway, samples with different hexanol concentrations were studied. Fig. 6a shows that the lifetime of BChl *c* in untreated chlorosomes (17 ps) is slightly shorter than that of BChl *c* in the 670 nm form (24 ps, Fig. 6c). In 48 mM hexanol (Fig. 6b), the chlorosome sample displayed almost equal absorption and fluorescence emission of the 670 and 730–740 nm band. However, the major fast energy transfer component from global analysis of single-photon counting experimental data was centered at 750 nm, with a relatively small band around 680 nm (Fig. 6b). A possible reason is that when 670 nm BChl *c* is excited by the 650 nm laser beam, excited state energy is transferred very rapidly to 730–740 nm BChl *c* and is therefore not resolvable in this experiment. The longer-wavelength 730–740 nm absorbing BChl *c* then decays in 10–20 ps.

Fig. 6d also shows that the amplitude ratio of the negative peak around 800 nm and the positive BChl *c* peak (around 680 nm) is considerably larger for the hexanol-containing samples as compared to untreated chlorosomes (Fig. 6a, 750 nm BChl *c* band). The overlap between the 750 nm BChl *c* and 800 nm BChl *a* fluorescence probably cancelled out some of the negative elements around 800 nm, resulting in a small BChl *a* negative peak. When the BChl *c* is partly or completely shifted

Table 2
Energy transfer efficiency (ETE, %) from different spectral forms of BChl *c* to BChl *a* 795 in native and hexanol-treated chlorosomes

	BChl *c* band	
[Hexanol] (mM)	670 nm	730–740 nm
0	N/A	58
48	36	38
56	24	30
68	13	N/A

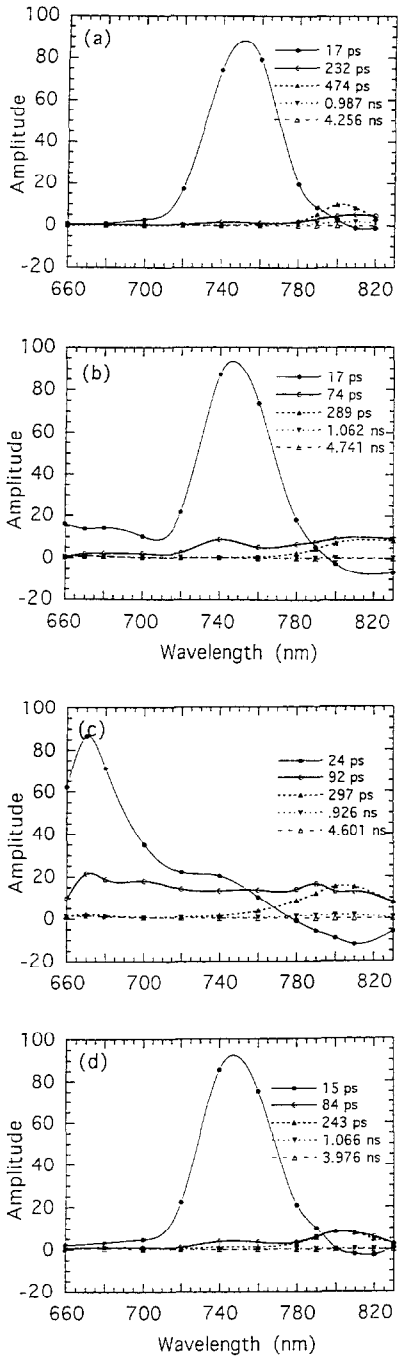

Fig. 6. Decay-associated emission spectra of untreated chlorosomes (a), chlorosomes in 48 mM (b) and 68 mM (c) hexanol, and in 34 mM hexanol after the 68 mM hexanol treatment (d). All the data were taken at room temperature (25°C) with excitation at 590 nm for (a), (d) and 650 nm for (b), (c), and were fitted with five components. The data points for the two longer-lifetime components are overlapped at some wavelengths.

to 670 nm absorption by hexanol, the overlap between BChl *c* and BChl *a* fluorescence decreases and a much clearer negative peak appears at 800 nm. An alternative explanation is that in native chlorosomes, the aggregated BChl *c* molecules are excitonically coupled and therefore the oscillation strength of BChl *c* 740 would be much higher than that of BChl *a* 795. This would make the decay amplitude of BChl *c* much larger than the rise amplitude of BChl *a*. In the hexanol-treated chlorosomes, however, the BChl *c* aggregate is somewhat disrupted by the hexanol, and the BChl *c* molecules would behave more like monomers. In this case, there would not be as great an amplitude difference in the decay of BChl *c* and the rise of BChl *a*, as compared to the native chlorosomes.

4. Discussion

We performed both contact and non-contact mode AFM on chlorosome samples. In all the AFM experiments, the chlorosome structures bound firmly to the mica plate, which mainly contains polar Si–O bonds with negative surface charge. Compared to electron microscopy (EM), one advantage of AFM is that sample preparation is rather easy. The sample does not need to be freeze-fractured as in most EM, but only needs to be air-dried at room temperature. Therefore, AFM is a potentially useful technique to image biological samples that are vulnerable to low temperature and high vacuum.

The length and width of the chlorosomes as measured by AFM agree rather well with values reported previously using EM. However, the height measurements are systematically smaller than those found using EM. Similar discrepancies in height measurements have been reported in AFM and STM studies on a variety of samples [47–49]. A possible reason is that when the vesicles settle on the mica surface, their shape is distorted due to the interaction between the structures and the mica. It has been reported before that the apparent thickness of a structure depends on the substrate it is adsorbed to [47]. Different interactions between the substrate and the sample can cause as much as 5 nm height difference. Instrumental artifacts could also be involved, complicating data analyses. Previous studies have reported similar height anomaly on biological samples by contact mode AFM. In one study, the height as measured by AFM was up to 10-fold lower than that by transmission electron microscopy (TEM) [48]. Numerous other factors could contribute to the height discrepancy. These include capillary effect and mechanical deformation due to the relative movement of the tip with respect to the sample [44].

From the contact mode AFM pictures (Fig. 4) of the SDS-treated chlorosomes, structures were rather flat, instead of spherical as previously reported [32]. For the native chlorosome sample, the average length (99 nm) and width (31 nm) are close to the dimensions measured by EM [6], whereas the height (5 nm), is only half of the height determined by EM. We used tapping mode AFM, in which case the influence of the lateral forces is greatly reduced. Some other factors, including carbon coating and adhesion to the substrate, may also affect height obtained by AFM. To make the sample robust, a 20 nm thick carbon coating was applied on the untreated chlorosomes.

The carbon coating, however, need not be evenly distributed on the surface. On the average, a 5% (of the carbon layer thickness) inaccuracy is introduced (John Wheatley, personal communication). Therefore, the chlorosome height has approximately a 1 nm uncertainty from the carbon coating. Another factor is the thickness distortion due to the interaction between the sample and the substrate. Mica, which has a negatively charged surface, was used in current AFM experiments, whereas carbon coated gold or copper grid with a neutral exterior was used in the previous EM measurements [6].

In order to fully understand the height discrepancy observed by AFM and EM, it will be necessary to obtain information about physical properties of chlorosomes, such as, elasticity and adhesion forces. Similar studies have been performed recently [50] to investigate the adsorption of lysozyme molecules on mica substrates. Future experiments that might resolve this question include tapping mode AFM in liquid samples. AFM experiments in liquid are expected to reduce the disruption of soft biological samples when imaged under ambient conditions [51] and to eliminate capillary forces [52].

When chlorosomes are diluted into hexanol-saturated buffer, the BChl *c* absorption band shifts from 740 to 670 nm. Our AFM pictures showed that the chlorosomes become much more rounded in shape and larger in overall size, with an estimated 5-fold increase in volume. Lehmann et al. [53] also observed an increase of chlorosome dimensions after hexanol treatment. The enlargement of the chlorosomes is probably due to the intake of hexanol molecules and the disruption of BChl *c* aggregates. Because hexanol has a six-carbon hydrophobic chain, it easily goes through the chlorosome lipid envelope and binds to the BChl *c* inside the chlorosomes. After this hexanol-treated sample is diluted into fresh buffer, it recovers most of the spectroscopic properties of untreated samples, judging from steady-state absorption and time-resolved fluorescence studies. However, neither the shape nor the volume of the chlorosomes returns to the original state. The hexanol concentration in this diluted solution was about 34 mM. If we assume that the amount of hexanol inside chlorosomes is proportional to the overall concentration in solution, there would still be about half as much hexanol in the chlorosomes after dilution. Therefore, the chlorosomes in this solution would be still much larger than those in a buffer with no hexanol at all. Because the interior of the chlorosome is somewhat hydrophobic, the hexanol molecules that have gone through the envelope may be 'trapped' inside this environment, which also makes the chlorosome shape remain rounded. Most of the hexanol molecules inside chlorosomes after dilution are probably not bound to any BChl *c* molecules, but either floating around between BChl *c* or mixed with the envelope lipid layer. So, although BChl *c* molecules convert back into the 740-nm-absorbing aggregates, they may still be surrounded by hexanol.

4.1. Pigment organization and energy transfer in hexanol-treated chlorosomes

Several studies have shown that BChl *c* in chlorosomes is highly ordered, with the Q_y electronic transition dipoles almost parallel to the long axis of the chlorosome [9,54–56]. Upon hexanol treatment, this Q_y orientation is lost according to LD measurements [40]. Hexanol, like many other alcohols, probably disrupts the normal BChl *c* aggregate structure by displacing BChl *c* 3^1-hydroxyl groups as ligands to the Mg atoms of adjacent molecules.

Our kinetic data from the picosecond fluorescence spectroscopic studies clearly demonstrated a fast energy transfer from BChl *c* to *a* in the hexanol-treated chlorosomes, with an excited state lifetime of 24 ps for BChl *c*. In terms of Förster energy transfer, it is somewhat surprising that such a fast energy transfer process exists, considering that there is virtually no spectral overlap between the BChl *c* 670 fluorescence emission band and BChl *a* 795 absorption band. Therefore, a direct Förster energy transfer is not likely, suggesting that another intermediate component of energy transfer might be involved. One possible candidate is the BChl *c* 730–740 species. Although the absorption spectrum of the chlorosomes in 68 mM hexanol does not show a peak in this region, the fluorescence emission spectrum does display a shoulder around 730 nm (Fig. 5d). Similar results were also shown by Matsuura and Olson [39]. This suggests the presence of a trace amount of an intermediate species of BChl *c*. In fact, the increasing ETE from 670 to 790 nm with higher BChl *c* 730–740 concentration also seemed to support an intermediate role of the 730–740 nm species. Therefore, our current fluorescence data suggest that when the BChl *c* 730–740 aggregate is present with the BChl *c* 670, at least part of the energy transfer from 670 nm to 795 nm goes through the BChl *c* 730–740 species.

The lifetime of the monomeric BChl *c* in the hexanol-treated samples is much shorter than the decay of free BChl *c* monomers, which is 6.5 ns in CH_2Cl_2 + 0.5% methanol [57]. The data shown in Fig. 6c clearly show that energy transfer to BChl *a* is responsible for part of the short lifetime, as discussed above. However, energy transfer is not the primary pathway for decay of the excited state. The energy transfer efficiency in the hexanol-treated chlorosomes is much lower than that in untreated ones, 13% vs 58%. This strongly suggests that a fast relaxation process which competes with the energy transfer has been introduced upon hexanol treatment. This additional quenching process is likely to be related to the well known phenomenon of concentration quenching, which has been extensively studied in chlorophyll systems for many years [58–61]. The bulk concentration of BChl *c* in the chlorosome is in the range of 0.3–1 M, depending on the precise values chosen for the volume and the number of BChl *c* per chlorosome, which in turn depend on growth conditions [62,63]. The concentration in the hexanol-treated

chlorosomes is almost certainly somewhat lower due to the swelling that takes place upon hexanol treatment. However, even with a substantial margin for error, the pigment concentration in hexanol-treated chlorosomes is well into the range that exhibits almost complete fluorescence quenching in chlorophyll solutions, vesicles or liposomes [60,61]. How the intact chlorosome avoids this fate is not yet understood, but is probably related to the strong exciton coupling in the native system.

Acknowledgements

We thank Dr. Daphna Yaniv for helping set up the AFM instrument and Dr. Gary Hastings for useful discussions. We also thank Drs. John Olson and Su Lin for reading the manuscript and giving helpful suggestions. This work was supported by grant DE-FG-85ER133388 (to R.E.B.) from the Division of Energy Biosciences of the U.S. Department of Energy. This is publication 241 from the Arizona State University Center for the Study of Early Events in Photosynthesis.

References

[1] Olson, J.M. (1980) Biochim. Biophys. Acta 594, 33–51.
[2] Holzwarth, A.R., Griebenow, K. and Schaffner, K. (1992) J. Photochem. Photobiol. A, 65, 61–71.
[3] Zuber, H. and Brunisholz, R. (1991) in Chlorophylls (Scheer, H., ed.), pp. 627–703, CRC Press, Boca Raton.
[4] Van Grondelle, R., Dekker, J.P., Gillbro, T. and Sundstrom, W. (1994) Biochim. Biophys. Acta 1187, 1–65.
[5] Blankenship, R.E., Olson, J.M. and Miller, M. (1995) in Anoxygenic Photosynthetic Bacteria (Blankenship, R.E., Madigan, M.T. and Bauer, C.E., eds.), pp. 399–435, Kluwer, Dordrecht.
[6] Staehelin, L.A., Golecki, J.R., Fuller, R.C. and Drews, G. (1978) Arch. Microbiol. 119, 269–277.
[7] Schmidt, K. (1980) Arch. Microbiol. 124, 21–31.
[8] Feick, R.G., Fitzpatrick, M. and Fuller, R.C. (1982) J. Bacteriol. 150, 905–15.
[9] Betti, J.A., Blankenship, R.E., Natarajan, L.V., Dickinson, L.C. and Fuller, R.C. (1982) Biochim. Biophys. Acta 680, 194–201.
[10] Feick, R.G. and Fuller, R.C. (1984) Biochemistry 23, 3693–3700.
[11] Brune, D.C., King, G.H., Infosino, A., Steiner, T., Thewalt, M.L.W. and Blankenship, R.E. (1987) Biochemistry 26, 8652–8658.
[12] Mimuro, M., Nozawa, T., Tamai, N., Shimada, K., Yamazaki, I., Lin, S., Knox, R.S., Wittmershaus, B.P., Brune, D.C. and Blankenship, R.E. (1989) J. Phys. Chem. 93, 7503–7509.
[13] Holzwarth, A.R., Müller, M.G. and Griebenow, K. (1990) J. Photochem. Photobiol. B, 5, 457–465.
[14] Causgrove, T.P., Brune, D.C., Wang, J., Wittmershaus, B.P. and Blankenship, R.E. (1990) Photosynth. Res. 26, 39–48.
[15] Miller, M., Cox, R.P. and Gillbro, T. (1991) Biochim. Biophys. Acta 1057, 187–194.
[16] Lin, S., Van Amerongen, H. and Struve, W.S. (1991) Biochim. Biophys. Acta 1060, 13–24.
[17] Müller, M.G., Griebenow, K. and Holzwarth, A.R. (1993) Biochim. Biophys. Acta 1144, 161–169.
[18] Van Noort, P.I., Francke, C., Schoumans, N., Otte, S.C.M., Aartsma, T.J. and Amesz, J. (1994) Photosynth. Res. 41, 193–203.
[19] Savikhin, S., Zhu, Y., Lin, S., Blankenship, R.E. and Struve, W.S. (1994) J. Phys. Chem. 98, 10322–10334.
[20] Alden, R.G., Lin, S.H. and Blankenship, R.E. (1992) J. Lumin. 51, 51–66.
[21] Van Dorssen, R.J. and Amesz, J. (1988) Photosynth. Res. 15, 177–189.
[22] Mimuro, M., Nozawa, T., Tamai, N., Nishimura, Y. and Yamazaki, I. (1994) FEBS Lett. 340, 167–172.
[23] Wechsler, T., Suter, F., Fuller, R.C. and Zuber, H. (1985) FEBS Lett. 181, 173–178.
[24] Niedermeier, G., Scheer, H. and Feick, R.G. (1992) Eur. J. Biochem. 204, 685–692.
[25] Griebenow, K. and Holzwarth, A.R. (1989) Biochim. Biophys. Acta 973, 235–240.
[26] Bystrova, M.I., Mal'gosheva, I.N. and Krasnovskii, A.A. (1979) Mol. Biol. 13, 582–594.
[27] Smith, K.M., Kehres, L.A. and Fajer, J. (1983) J. Am. Chem. Soc. 105, 1387–1389.
[28] Brune, D.C., Nozawa, T. and Blankenship, R.E. (1987) Biochemistry 26, 8644–8652.
[29] Olson, J.M. and Pedersen, J.P. (1990) Photosynth. Res. 25, 25–37.
[30] Hirota, M., Moriyama, T., Shimada, K., Miller, M., Olson, J.M. and Matsuura, K. (1992) Biochim. Biophys. Acta 1099, 271–274.
[31] Miller, M., Gillbro, T. and Olson, J.M. (1993) Photochem. Photobiol. 57, 98–102.
[32] Miller, M., Simpson, D. and Redlinger, T.E. (1993) Photosynth. Res. 35, 275–283.
[33] Blankenship, R.E., Brune, D.C., Freeman, J.M., King, G.H., McManus, J.D., Nozawa, T., Trost, J.T. and Wittmershaus, B.P. (1988) in Green Photosynthetic Bacteria (Olson, J.M., Ormerod, J.G., Amesz, J., Stackebrandt, E. and Trüper, H.G., eds.), pp. 57–68, Plenum, New York.
[34] Lutz, M. and Van Brakel, G. (1988) in Green Photosynthetic Bacteria (Olson, J.M., Ormerod, J.G., Amesz, J., Stackebrandt, E. and Trüper, H.G., eds.), pp. 23–34, Plenum, New York.
[35] Brune, D.C., King, G.H. and Blankenship, R.E. (1988) in Photosynthetic Light-Harvesting Systems (Scheer, H. and Schneider, S., eds.), pp. 141–151, Walter de Gruyter, Berlin.
[36] Holzwarth, A.R. and Schaffner, K. (1994) Photosynth. Res. 41, 225–233.
[37] Nozawa, T., Ohtomo, K., Suzuki, M., Nakagawa, H., Shikama, Y., Konami, H. and Wang, Z.Y. (1994) Photosynth. Res. 41, 211–223.
[38] Hildebrandt, P., Tamiaki, H., Holzwarth, A.R. and Schaffner, K. (1994) J. Phys. Chem. 98, 2192–2197.
[39] Matsuura, K. and Olson, J.M. (1990) Biochim. Biophys. Acta 1019, 233–238.
[40] Matsuura, K., Hirota, M., Shimada, K. and Mimuro, M. (1993) Photochem. Photobiol. 57, 92–97.
[41] Binning, G., Quate, C.F. and Gerber, C.H. (1986) Phys. Rev. Lett. 56, 930–933.
[42] Pierson, B.K. and Castenholz, R.W. (1992) in The Prokaryotes (Balows, A., Trüper, H.G., Dworkin, M., Schliefer, K.H. and Harder, W., eds.), pp. 3754–3774, Springer, Berlin.
[43] Gerola, P.D. and Olson, J.M. (1986) Biochim. Biophys. Acta 848, 69–76.
[44] Zhong, Q., Inniss, D., Kjoller, K. and Elings, V. (1993) Surface Sci. Lett. 290, 688–692.
[45] Causgrove, T.P., Brune, D.C., Blankenship, R.E. and Olson, J.M. (1990) Photosynth. Res., 25, 1–10.
[46] Van Dorssen, R.J., Vasmel, H. and Amesz, J. (1986) Photosynth. Res. 9, 33–45.
[47] Butt, H.-J., Downing, K.H. and Hansma, P.K. (1990) Biophys. J. 58, 1473–1480.
[48] Eppell, S.J., Zypman, F.R. and Marchant, R.E. (1993) Langmuir 8, 2281–2288.

[49] Imai, K., Yoshimura, K., Tomitori, M., Nishikawa, O., Kokawa, R., Yamamoto, M., Kobayashi, M. and Ikai, A. (1993) Jpn. J. Appl. Phys. 32, 2962–2964.
[50] Radmacher, M., Fritz, M., Cleveland, J.P., Walters, D.A. and Hansma, P.K. (1994) Langmuir 10, 3800–3814.
[51] Weisenhorn, A.L., Hansma, P.K., Albrecht, T.E. and Quate, C.F. (1989) Appl. Phys. Lett. 54, 2651–2654.
[52] Weisenhorn, A.L., Maivald, D., Butt, H.-J. and Hansma, P.K. (1992) Phys. Rev. B45, 11226–11231.
[53] Lehmann, R.P., Brunisholz, R.A. and Zuber, H. (1994) Photosynth. Res. 41, 165–173.
[54] Van Amerongen, H., Vasmel, H. and Van Grondelle, R. (1988) Biophys. J. 54, 65–76.
[55] Van Amerongen, H., Van Haeringen, B., Van Gurp, M. and Van Grondelle, R. (1991) Biophys. J. 59, 992–1001.
[56] Griebenow, K., Holzwarth, A.R., Van Mourik, F. and Van Grondelle, R. (1991) Biochim. Biophys. Acta 1058, 194–202.
[57] Brune, D.C., Blankenship, R.E. and Seely, G.R. (1988) Photochem. Photobiol. 47, 759–763.
[58] Livingston, R., Watson, W.F. and McArdle, J. (1949) J. Am. Chem. Soc. 71, 1542–1550.
[59] Gutschick, V.P. (1978) J. Bioenerget. Biomembr. 10, 153–170.
[60] Beddard, G.S. and Porter, G. (1976) Nature 260, 366–367.
[61] Beddard, G.S., Carlin, S.E. and Porter, G. (1976) Chem. Phys. Lett. 43, 27–32.
[62] Golecki, J.R. and Oelze, J. (1987) Arch. Microbiol. 148, 236–241.
[63] Oelze, J. and Golecki, J.R. (1995) in Anoxygenic Photosynthetic Bacteria (Blankenship, R.E., Madigan, M.T. and Bauer, C.E., eds.), pp. 259–278, Kluwer, Dordrecht.